2013 IEEE International Conference on Systems, Man, and Cybernetics

A Measuring and Analysis Method of Coupled Range of Motion of the Human Hands

Natsuki Miyata
Digital Human Research Center
AIST
Tokyo, JAPAN
n.miyata@aist.go.jp

Yuki Shimizu
Div. of Systems Integration,
Graduate School of Engineering,
Yokohama National University
Kanagawa, JAPAN

Yusuke Maeda
Div. of Systems Research,
Faculty of Engineering,
Yokohama National University
Kanagawa, JAPAN

***Abstract*—This paper proposed a method of modeling the range of motion (ROM) of the human hand, which has multiple joints that move in coordination. Traditionally, ROM of the hand was defined by independently bounding each joint angle from observation of extreme posutres. For example, the joint angle when fully extended (maximum) and that when fully flexed (minimum) were observed. However, it is difficult to express actual human's complex ROM with such simple boundaries. Therefore, we modeled ROM of the hand by defining outer boudary of collected various posture data. Each relationship between two of the joint angles was presented as a united area in which all the projected measured postures on the plane were minimally bounded using the α-convex hull algorithm. Such area was called "a coupled ROM" in this paper. Measurement and modeling experiments on four subjects were conducted to demonstrate basic characteristics of the proposed ROM model. The occupied volume of the proposed ROM was compared with that of the simple upper-lower ROM. The coordinatinated relationships were ranked and categorized for comparison among subjects.**

***Keywords*—Joint range of motion, Joint coupling, human hand**

I. INTRODUCTION

The human hand is a multidimensional system that has about 20 joints that move in coordination with each other. Recent motion measurement apparatus have facilitated the observation of whole hand motions and accelerated studies on the coordinated motion of the joints. Beyond formulating a well-known relationship between the proximal and the distal interphalangeal (PIP and DIP) joints [11], many studies have investigated the synergy of the joints when reaching to grasp or manipulating objects ([7]-[10]). Some have tried to mechanically model the joint couplings in each finger ([12], [13]). Such studies can be further developed if discussed with the range of motion (ROM) of the hand, which is one of the basic properties used for posture assessments. For example, a synthesized posture of a human hand is considered natural or feasible if it satisfies the criteria of the standard ROM. In a product design with human models (e.g., [1]), the ROM is used to estimate the reachability of the extremities (for example, the fingertip or thumbtip) and the ergonomic comfort of the posture because human beings often feel uncomfortable in extreme postures.

Traditionally, the ROM of the hand was modeled independently for each joint angle neglecting inter-joint coordination. Using a goniometer, two oppositely-extreme postures (for example, fully extended and fully flexed) were measured ([2]-[6]). Hand joints do not move independently, but in coordination, due to the anatomy or innervation. Therefore, it is difficult to express the complex ROM of the actual hand by such simple boundaries.

Hence, we propose a method to model range of coordinated motion as "a coupled ROM" by collecting an adequate variety of whole hand motions. This is premised on the idea that ROM is a set of all the feasible hand postures enabled by joint coupling.

An overview of our modeling method is presented in the next section, after which we present in sections III and IV posture measurements and ROM modeling experiments that we carried out on four subjects.

II. COUPLED V.S. INDEPENDENT ROM

The human hand is a multidimensional system that consists of many joints and its posture is expressed with multiple variables. It is difficult to directly deal with all the couplings among the joints at the same time. We therefore propose a model of the range of motion of the whole hand as a set of all the relationships between two of the posture variables (Fig. 1). If a hand posture is expressed with n posture variables $q_i (i = 1, \ldots, n)$, ${}_nC_2$ relationships exist, where ${}_nC_2$ is the number of all the possible two-fold combination of the variables. In the case of a joint with a single degree of freedom, it is simple and preferable to consider the joint angle around the joint axis as a posture variable. In the case of a joint with multiple degrees of freedom, three rotational angles around the local coordinate axes can be employed to simply express its complex motion precisely. Even the degrees of freedom in terms of controllability is two, the number of posture variables is not necessarily equal to that because such dependency among posture variables are also treated as coordination.

Let us consider the relationships between q_i and q_j. Assuming that an adequate variety of posture data can be collected, they can be used to form the ROM of q_i and q_j when projected on the $q_i q_j$ plane. In this plane, the classic ROM defined by the minimum and maximum joint angles (hereafter "upper-lower boundary ROM") corresponds to a rectangle as shown in Fig. 2. If no coordination exists between q_i and q_j, the projected data points will be located all over the rectangle.

978-1-4799-0652-9/13 $31.00 © 2013 IEEE
DOI 10.1109/SMC.2013.448

However, if a strong coordination exists, the data points will be located in a limited area within the rectangle, which is the reason why the classic ROM includes impossible postures. We therefore propose to express the boundary of the area in which the projected data points are located to model ROM that reflects joint coupling. We call this a "coupled ROM" hereafter.

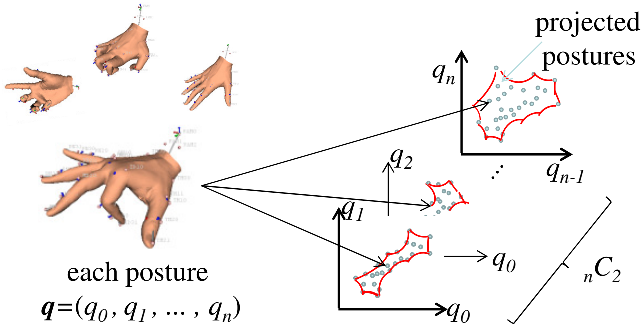

Fig. 1. Overview of our ROM modeling method

Since the projected data points might form a complex shape, we use the α-convex hull [15], an extended convex hull that allows non-convex shape, to express the area as precisely as possible. The α-convex hull is the space $C_\alpha(A)$ that satisfies the following condition:

$$C_\alpha(A) = \bigcap_{\{\mathring{B}(x,\alpha):\, \mathring{B}(x,\alpha)\cap A=\emptyset\}} \left(\mathring{B}(x,\alpha)\right)^c, \qquad (1)$$

where $\mathring{B}(x,\alpha)$ represents an open sphere with origin x and radius α, and $(\mathring{B}(x,\alpha))^c$ is a complement of $\mathring{B}(x,\alpha)$.

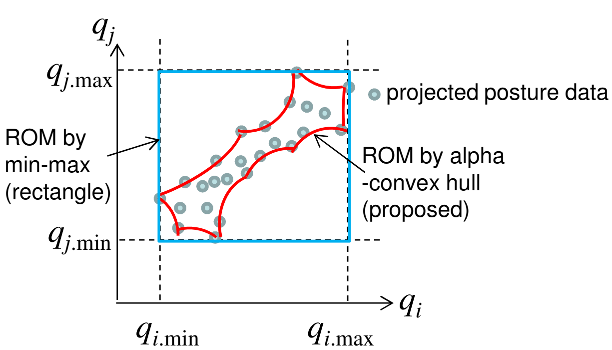

Fig. 2. Range of motion in each two dimensional plane(a coupled ROM for q_i and q_j)

III. Hand posture measurement for ROM modeling

A. Hand motion capture

To confirm the effectiveness of the proposed model system, we collected the hand motions of four male subjects (young and healthy adults). The hand motions were measured using the optical motion capture system Vicon MX. The captured marker positions were converted into posture data using the method in [14]. The method constructs the individual hand model of a subject – showing the surface shape and the skeleton – by scaling a generic model in Fig. 3, which uses 29 posture variables to express the whole posture. In this hand model, the wrist joint, the carpometacarpal (CM) joint of the thumb, and the metacarpophalangeal (MP) joints of the other fingers respectively use three posture variables to efficiently express the actual movements of the joint that has two degrees of freedom controlability. This results in a correlation among the three posture variables in each joint.

Fig. 4 shows some examples of the captured and reconstructed postures of Subject 1, which suggests that the model works well in reconstructing the original motion.

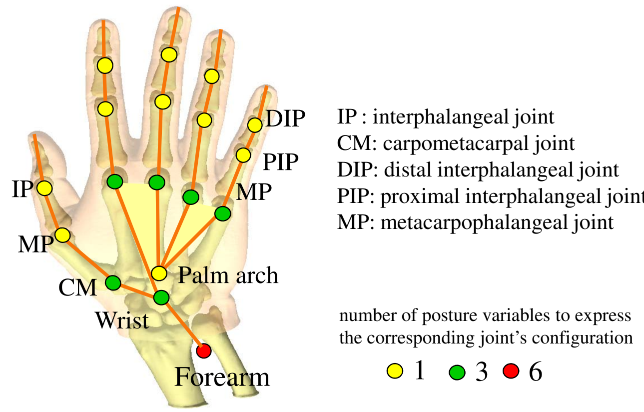

Fig. 3. Joints in a human hand and a generic hand model for processing captured marker positions with the number of posture variables

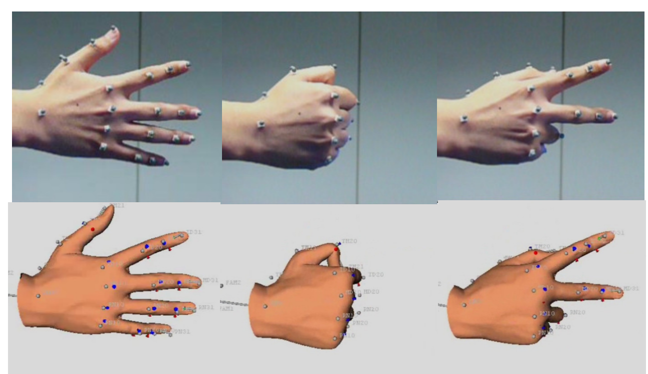

Fig. 4. Examples of the reconstructed postures(lower row) with the actual hand of Subject 1(upper row)

B. Contents of measurement

In our preliminary experiment, we observed that the subjects could not move widely across their ROM when instructed to "move arbitrarily." Furthermore, it was necessary to evenly spread the variety of motions among the subjects as much as possible for proper comparison. Therefore, we gave them the same set of exercises summarized in Table I. Some snapshots are shown in Fig. 5. These exercises were selected to include various joint postures both in the middle and on the boundary. The subjects were instructed orally and by demonstration on how to execute the exercises with the appropriate speed. Each exercise was then captured after adequate practice.

TABLE I. 21 EXERCISES FOR DEVELOPING THE COUPLED ROM

e1	Flexion and extension of all the joints at the same time
e2	Abduction and adduction of all the joints at the same time
e3	Flexion and extension of the joints of each finger independently
e4	Abduction and adduction of the joints of each finger independently
e5	Rock-paper-scissors
e6	Random wiggle for five seconds
e7	Flexion and extension of the thumb and all the fingers at the same time with one of the fingers flexed
e8	Flexion of only PIP and DIP joints
e9	Flexion and extension of the thumb and the fingers with one of the fingers' PIP and DIP joint flexed
e10	Flexion and extension of the thumb and all the fingers with the wrist extended
e11	Flexion and extension of the thumb and all the fingers with the wrist flexed
e12	Flexion of the MP joint of each finger, followed by flexion of the PIP joint
e13	Flexion of the MP joints of all the fingers at the same time
e14	Flexion of the MP joints of all the fingers at the same time, followed by flexion of the PIP joints
e15	Posture to grasp a ball
e16	Clockwise rotation of the MP joint of each finger
e17	Counterclockwise rotation of the MP joint of each finger
e18	Flexion of the PIP and DIP joints from the thumb to the little finger and extension in the reverse order
e19	Flexion of the whole thumb and each finger from the thumb to the little finger and extension in the reverse order
e20	Flexion of the PIP and DIP joints from the little finger to the thumb and extension in the reverse order
e21	Flexion of the thumb and the fingers independently from the little finger and extension in the reverse order.

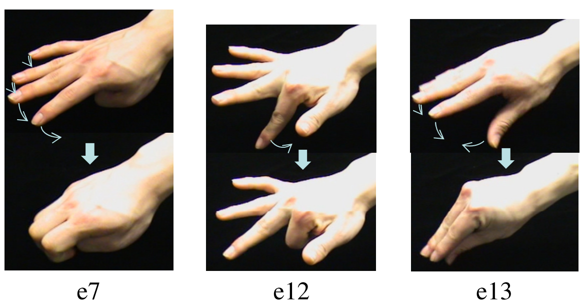

Fig. 5. Snapshots of three of the exercises in Table I

IV. RANGE OF MOTION MODEL FROM THE MEASUREMENT

A. Extracted Range of Motion

Before extracting all the coupled ROMs, the value of the parameter of α-convex hull (α) was determined. To determine the range of motion with the precise border of the measured data distribution, it is preferable to set a small value of α. However, a value of α that is too small sometimes results in an undesirable void inside the united area as shown in Fig. 6 (a). Such a void is prone to appear when the captured motions do not cover the actual range of motion evenly and should be avoided to appear. Through trial and error, we determined the suitable value to be $30[\text{deg}]$ (Fig. 6 (b)), which was confirmed by the disappearance of the void. The occurence of such voids can be reduced by improving the set of exercises given to the subjects, which we intend to do in a future works.

Since we used a hand model with 29 posture variables (Fig. 3), 406 (i.e., ${}_{29}C_2$) coupled ROMs were derived to form the proposed ROM. Fig.7 shows some typical coupled ROMs. Fig.7 (a) shows the relationship between the PIP and DIP joints, the coordinated behaviour of which is well known. Some projected posture data existed in the limited area, indicating that the postures of these joints were strongly coupled to each other. Fig.7 (b) shows the relationship between the MP joints of the adjacent fingers. The strengh of coupling is weaker than that shown in Fig.7 (a) but a certain joint coupling was observed. The opposite pattern of the coupled ROM is shown in Fig. 7(d). The strength of the coupling is very low and the posture data are scattered over the rectangle defined by the upper-lower boundary ROM. Unlike the foregoing three, Fig. 7(c) shows the directed coupling. In this case, the PIP joint of the ring finger was affected by the posture of the PIP joint of the little finger, but it was not affected in the reverse direction. In other words, the PIP joint of the little finger can move independently of the PIP joint of the ring finger.

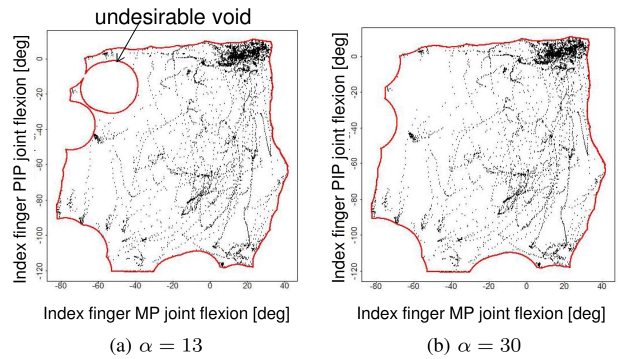

Fig. 6. Difference of α value and the resulted α-convex hull. Dark spots represent all the measured postures.

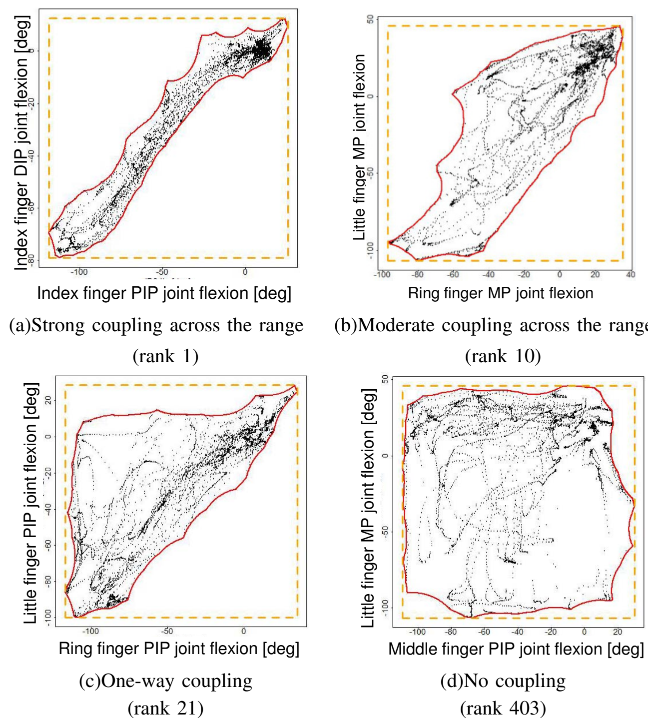

Fig. 7. Selected coupled ROMs of Subject 1 with ranks by index Coord

The quantitative difference between the proposed coupled

ROMs and the upper-lower boundary ROM was figured out with the estimated volume. As expected, it was estimated that the proposed coupled ROM occupied a smaller volume than the classic upper-lower boundary ROM (see Table II for a summary). The results showed that the coupled ROM occupied a compact space of about $1/10^6$ that of the classic upper-lower boundary ROM. The occupied volume was estimated as described below.

The volume of the upper-lower boundary ROM $V_{\rm all}$ was estimated as follows:

$$V_{\rm all} = \prod_{i \in \mathbf{Q}_s} (q_{i.\max} - q_{i.\min}), \tag{2}$$

where $\mathbf{Q}_s$ is a set of posture variables considered in the analysis. The maximum and minimum values of the posture variable q_i ($q_{i.\max}$ and $q_{i.\min}$) were obtained from the measured postures.

Concerning the ROM volume estimation for the proposed coupled ROMs, we first tried Monte Carlo method but no randomly generated sample (posture) satisfied the coupled ROMs even after 10^8 trials, which ends as the volume is zero. We therefore estimated the maximum ROM volume of the proposed coupled ROM alternatively by solving the following relation:

$$(1 - V_{\rm c_{free.p}}/V_{\rm all})^{N_{\rm s}} \geq p_{\rm c}. \tag{3}$$

This equation indicates that the probability that none of the $N_{\rm s}$ generated samples is included in the range of motion is at least $p_{\rm c}$. Based on the above trial fact, $N_{\rm s}$ and $p_{\rm c}$ were fixed at 10^8 and 0.01, respectively.

TABLE II. ESTIMATED ROM VOLUME WITH ALL 29 VARIABLES

Subjects	$V_{\rm c_{free,P}}[\rm rad^{29}]$	$V_{\rm all}[\rm rad^{29}]$	$V_{\rm c_{free,p}}/V_{\rm all}$
subject 1	$\leq 1.6\times10^{-4}$	349	4.6×10^{-7}
subject 2	$\leq 2.8\times10^{-4}$	627	4.5×10^{-7}
subject 3	$\leq 3.4\times10^{-2}$	73214	4.6×10^{-7}
subject 4	$\leq 1.2\times10^{-5}$	26	4.6×10^{-7}

B. Coordination of the joints

To study the coordination of the joints of the hand, we ranked the coulpled ROMs by an index Coord that we defined as follows:

$$\mathrm{Coord} = \mathrm{Dim} + \mathrm{Flat} + R. \tag{4}$$

- $\mathrm{Dim} = 1 - S_1/S_2$ (where S_1 is the area of the α-convex hull and S_2 is the area of the rectangle formed by the minimum and maximum values of each posture variable that composes the coupled ROM).
- $\mathrm{Flat} = 1 - b/a$ (where a, b are respectively the lengths of the major and minor axes of the 95% probability ellipse of the scattered projected posture data that form the coupled ROM).
- R is the coefficient of determination of linear regression between two posture variables that compose the coupled ROM.

Dim is the area reduction of the proposed coupled ROM relative to that of the upper-lower boundary ROM. Flat is the oblateness of the probability ellipse that shows the unevenness of the posture data distribution. R shows the strength of the statistical correlation.

The ranks shown with typical coupled ROMs in Fig. 7 suggest that the index can show the gross tendency of the coordination strength.

Table III shows the top 12 coupled ROMs for Subject 1, ranked using the above index Coord and Table IV shows the top 12 coupled ROMs for other three subjects. The observed coordinations for all the subjects can be categorized as follows:

0) Coordination between two of the posture variables that describes the configuration of the same joint(e.g., ranks 5, 8, and 11 for Subject 1).
1) Coordination between the PIP and DIP joints in the same finger(e.g., ranks 1-3 and 4 for Subject 1).
2) Coordination between the palmar arch and the flexion of the MP joints(e.g., ranks 6 and 7 for Subject 1).
3) Coordination between the MP joints of adjacent fingers(e.g., ranks 9 and 10 for Subject 1).
4) Coordination between the wrist and the MP joint of the index finger in flexion/extension(e.g., rank 12 for Subject 1).
5) Coordination between the joint of the ring finger and that of the little finger(e.g., rank 2, 5, and 8 for Subject 2).
6) Coordination between the MP joint and the rest of the joints of the same finger(e.g., rank 4, 11, and 12 for Subject 2).

The category 0) is due to the hand model's posture variable definition. For example, our hand model describes the motion of MP joint that has two degrees of freedom in terms of controlability with three posture variables. There are therefore dependency among these three posture variables and the dependency appeared as corrdination. The rest of the categories, including the well-known coordination between the PIP and DIP joints (the category 1)), are appropriate from the view point of the anatomy and kinematics of the hand.

A comparison of tables III and IV shows that the coordination categories are similar among subjects, although the top 12 coordinations were not exactly the same.

C. Discussion

The experimental results showed the effectiveness of the proposed modeling method. To investigate the individuality and commonality of the derived joint coupling, it is necessary to ascertain if the current set of exercises is sufficient, since our method assumes an adequate variety of motions. However, from a practical point of view, it is important to moderate the amount of exercises to avoid wearing out the subjects. An index of coupling better than the Coord proposed in this paper can then be investigated.

Now let us show the possible contributions of the proposed coupled ROMs. The proposed ROM model can be used to generate feasible postures. Fig. 8 includes the randomly generated postures that satisfy the given ROM. With a classic upper-lower

TABLE III. TOP 12 COORDINATIONS FOR SUBJECT 1

rank	coupled posture variables		Dim	Flat	R	Coord	coordination category
1	Index finger PIP joint flexion	Index finger DIP joint flexion	0.80	0.90	0.98	0.89	1
2	Little finger PIP joint flexion	Little finger DIP joint flexion	0.78	0.88	0.97	0.88	1
3	Middle finger PIP joint flexion	Middle finger DIP joint flexion	0.79	0.87	0.97	0.87	1
4	Ring finger PIP joint flexion	Ring finger DIP joint flexion	0.66	0.82	0.93	0.80	1
5	Index finger MP joint flexion	Index finger MP joint pronation	0.66	0.86	0.83	0.78	0
6	Palm arch	Little finger MP joint flexion	0.49	0.97	0.74	0.73	2
7	Palm arch	Index finger MP joint flexion	0.54	0.95	0.68	0.72	2
8	Thumb CM joint flexion	Thumb CM joint abduction	0.66	0.69	0.82	0.72	0
9	Ring finger MP joint abduction	Little finger MP joint abduction	0.72	0.67	0.77	0.72	3 (5)
10	Ring finger MP joint flexion	Little finger MP joint flexion	0.57	0.73	0.85	0.72	3 (5)
11	Thumb CM joint flexion	Thumb CM joint pronation	0.75	0.63	0.74	0.71	0
12	Wrist flexion	Index finger MP joint flexion	0.63	0.78	0.70	0.71	4

boundary ROM, infeasible postures were frequently generated (Fig. 8 (a)). However, with the proposed coupled ROMs (the top 100 coupled ROMs of the previous chapter's "Coord"), most of the synthesized postures were feasible for the same subject as shown in Fig. 8(b). Note must be made that the coupled ROMs cannot completely eliminate infeasible postures because of self interference caused by non-adjacent joints. So a function to check self interference can be added to guarantee posture feasibility though we have not implemented because such self interference is very rare. Considering the fact that not all the joints move in coordination with others, it is advisable to selectively use coupled ROMs on the basis of the strength of coordination as shown in the previous chapter. Combined with other posture generation methods, the selective application might accelerate the process.

It would be interesting to combine our coupled ROM with previous findings about synergies. The analyzed principal components can be plotted as routes or vector fields on the relevant coupled ROM planes. An analysis of such principal components and the boundaries would afford a deeper understanding of mechanical and physiological aspects of synergy. Furthermore, considering recent use of principal component analysis in the field of robotics to synthesize grasping posture (for example, [16] and [17]), such combined information would facilitate posture synthesis since derived principal components are not sufficient for guaranteeing the feasibility of the postures.

To analyze the hand motion with external force when grasping or clibming, it would be better to additionally include such motion set in the coupled ROMs experiment. The range of motion would be slightly expanded when an external force is applied compared with that from the unloaded hand motion as done in this paper. Such is called a passive range of motion, which could not be actively posed by the subject. It is preferable to deal with the data sets of active and passive ranges of motion separately.

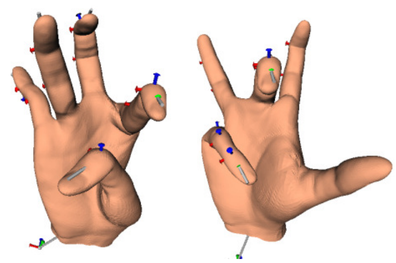

(a) Postures generated within classic upper-lower boundary ROM. Most of the results were infeasible for the subject.

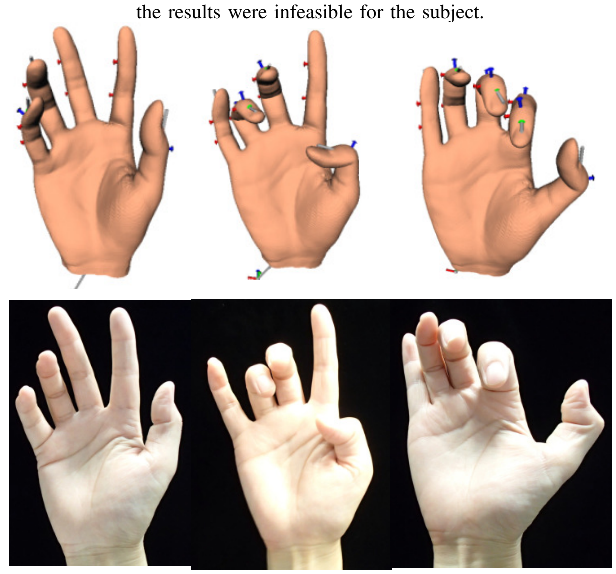

(b) Postures generated within the proposed coupled ROMs (upper row). Photos of the actual hand of the subject trying to pose them(lower row) show their feasibility.

Fig. 8. Examples of random posture generation

V. CONCLUSIONS

This paper proposed a method of modeling the feasible hand range of motion by determining appropriate boundary from a variety of measured postures. For a hand with N posture variables, our ROM model was defined as a set of ${}_NC_2$ two-dimensional regions (coupled ROMs) that describe the relationships between two of the posture variables. Each coupled ROM was derived as a united area that covers all the measured posture data points projected on the plane using the α-convex hull algorithm. The measurement and modeling experiments on four subjects showed the propriety of the proposed modeling method to build coupled ROMs. The volume of the coupled ROMs was about $1/10^6$ that of the upper-lower boundary ROM, which was because the former appropriately excluded most of the impossible postures of the latter. Some examples of the coupled ROMs showed the typical coordination patterns. When the joints moved in strong coordination, the projected data points were located in the limited area, which means the joints are in bidirectional coupling relation. Oppositely in the

TABLE IV. TOP 12 COORDINATION FOR THE OTHER SUBJECTS (R: RANK WITHIN THE SUBJECT, C: COORDINATION CATEGORY)

R	coupled posture variables		C
Subject 2			
1	Index finger PIP joint flexion	Index finger DIP joint flexion	1
2	Ring finger PIP joint flexion	Little finger PIP joint flexion	5
3	Middle finger MP joint flexion	Middle finger MP joint abduction	0
4	Thumb CM joint pronation	Thumb MP joint flexion	6
5	Ring finger MP joint pronation	Little finger DIP joint flexion	5
6	Ring finger MP joint flexion	Little finger MP joint flexion	3
7	Little finger PIP joint flexion	Little finger DIP joint flexion	1
8	Ring finger DIP joint flexion	Little finger DIP joint flexion	5
9	Middle finger PIP joint flexion	Middle finger DIP joint flexion	1
10	Ring finger PIP joint flexion	Ring finger DIP joint flexion	1
11	Index finger MP joint pronation	Index finger PIP joint flexion	6
12	Ring finger MP joint pronation	Ring finge PIP joint flexion	6
Subject 3			
1	Index finger PIP joint flexion	Index finger DIP joint flexion	1
2	Middle finger MP joint flexion	Middle finger MP joint abduction	0
3	Index finger MP joint flexion	Middle finger MP joint flexion	3
4	Middle finger MP joint abduction	Ring finger MP joint flexion	3
5	Middle finger MP joint flexion	Ring finger MP joint flexion	3
6	Middle finger MP joint pronation	Middle finger PIP joint flexion	6
7	Little finger PIP joint flexion	Little finger DIP joint flexion	1
8	Ring finger MP joint flexion	Little finger MP joint flexion	5
9	Ring finger PIP joint flexion	Ring finger DIP joint	1
10	Index finger MP joint flexion	Middle finger MP joint abduction	3
11	Wrist flexion	Middle finger MP joint flexion	4
12	Index finger MP joint flexion	Ring finger MP joint flexion	3
Subject 4			
1	Little finger PIP joint flexion	Little finger DIP joint flexion	1
2	Index finger PIP joint flexion	Index finger DIP joint flexion	1
3	Thumb MP joint flexion	Thumb IP joint flexion	6
4	Middle finger PIP joint flexion	Middle finger DIP joint flexion	1
5	Ring finger DIP joint flexion	Little finger PIP joint flexion	5
6	Ring finger DIP joint flexion	Little finger DIP joint flexion	5
7	Thumb CM joint pronation	Thumb MP joint flexion	6
8	Index finger MP joint pronation	Index finger PIP joint flexion	6
9	Ring finger PIP joint flexion	Ring finger DIP joint flexion	1
10	Middle finger MP joint flexion	Middle finger MP joint pronation	0
11	Middle finger MP joint flexion	Ring finger MP joint flexion	3
12	Index finger MP joint pronation	Index finger DIP joint flexion	6

case of the combination of the joints that move in very low coordination, the points were scattered all over the rectangle defined by the classic upper-lower boundary ROM. In some cases, the data points were located in a triangle, which means the joints are in one-way coupling relation. All the coupled ROMs were ranked with the index Coord defined in this paper and the highly ranked coordinated relationships were compared among subjects. Though the coordinated combinations of posture variables were not exactly the same among subjects, the included categories were similar.

To use our method in building a comprehensive ROM model based on massive measurements as in [2]-[6], we need to confirm propriety of the sets of exercises. We also need a coordination index that will enable us to judge if the measurements taken are reliable enough for forming an appropriate ROM. These are part of our future works. We believe that our coupled ROMs that express how well pairs of joints are coupled provide useful findings for future physiological studies and robotic/control researches.

ACKNOWLEDGMENT

This work was supported by KAKENHI 23700242 and 25330313.

REFERENCES

[1] N. Miyata, M. Kouchi, and M. Mochimaru, “Posture Estimation for Design Alternative Screening by DhaibaHand - Cell Phone Operation”, Proc. SAE 2006 Digital Human Modeling for Design and Engineering Conference, 2006-01-2327, 2006.

[2] J. C. Becker and N. V. Thakor, “A Study of the Range of Motion of Human Fingers with Application to Anthropomorphic Designs”, IEEE Transactions on Biomedical Engineering, Vol. 35, No. 2, 110-117, 1988.

[3] T. Shimada and S. Takemasa, “Normal Range of Motion of Joints in Young Japanese People,” Bulletin of allied medical sciences Kobe, Vol.4, 103-109, 1988.

[4] M. C. Hume, H. Gellman, H. McKellop, and R. H. Brumfield, Jr., “Functional Range of Motion of the Joints of the Hand”, The Journal of Hand Surgery, Vol. 15A, No. 2, 240-243, 1990.

[5] W. J. Mallon, H. R. Brown, and James A. Nunley, “Digital Ranges of Motion: Normal Values in Young Adults,” The Journal of Hand Surgery, Vol.16A, No.5, 882-887, September, 1991.

[6] B. Škvařilová, A. Plevková, “Ranges of Joint Motion of the Adult Hand”, Acta Chirurgiae Plasticae, Vol. 38, No. 2, 67-71, 1996.

[7] M. Santello, M. Flanders, and J.F. Soechting, “Postural Hand Synergies for Tool Use”, The Journal of Neuroscience, Vol. 18, No. 23, 10105-10115, 1998.

[8] C. R. Mason, J. E. Gomez, and T. J. Ebner, “Hand Synergies During Reach-to-Grasp”, Journal of Neurophysiology, Vol. 86, 2896-2910, 2001.

[9] E. Todorov, and Z. Ghahramani, “Analysis of the synergies underlying complex hand manipulation”, Proceedings of The 26th IEEE Annual International Conference on Engineering in Medicine and Biology Society, EMBC 2004, Vol. 6, 4637-4640, 2004

[10] J. N. Ingram, K.P. Körding, I.S. Howard, D.M. Wolpert, “The statistics of natural hand movements”, Experimental Brain Research 188, 223-236, 2008.

[11] H. Rijpkama and Michael Girard, “Computer Animation of Knowledge-Based Human Grasping,” ACM SIGGRAPH Computer Graphics, Vol. 25, No.4, 339-348, July, 1991.

[12] J. N. A. L. Leijnse, P. M. Quesada, and C. W. Spoor, “Kinematic Evaluation of the Finger’s Interphalangeal Joints Coupling Mechanism - Variability, Flexion-Extension Differences, Triggers, Locking Swanneck Deformities, Anthropometric Correlations”, Journal of Biomechanics, Vol. 43, 2381-2393, 2010

[13] J. N. A. L. Leijnse and C. W. Spoor, “Reverse Engineering Finger Extensor Apparatus Morphology from Measured Coupled Interphalangeal Joint Angle Trajectories - a Generic 2D Kinematic Model”, Journal of Biomechanics, Vol. 45, 569-578, 2012

[14] N. Miyata, Y. Motoki, Y. Shimizu, and Y. Maeda, “Individual Hand Model to Reconstruct Behavior from Motion Capture Data”, Proc. of the IEEE Int. Conf. Robotics and Automation, 1951-1956, 2011.

[15] B. Pateiro-Lopez and A. Rodriguez-Casal, “Generalizing the Convex Hull of a Sample: The R Package alphahull,” Journal of Statistical Software, Vol. 34, No. 5, 1-28, 2010.

[16] H. B. Amor, G. Heumer, B. Jung and A. Vitzthum, “Grasp Synthesis from Low-Dimensional Probabilistic Grasp Models”, Computer Animation and Virtual Worlds, Vol. 19, 445-454, 2008.

[17] M. T. Ciocarlie and P. K. Allen, “Hand Posture Subspaces for Dexterous Robotic Grasping”, IJRR, Vol. 28, No. 7, 851-867, 2009.